Dynamics of a Polyphosphazene Melt Studied by Solid-State ^{2}H NMR

Barbara Koch

Institut für Physikalische Chemie, Westfälische Wilhelms-Universität Münster, Corrensstr. 30, 48149 Münster, Germany

Michael Vogel*

Institut für Festkörperphysik, Technische Universität Darmstadt, Hochschulstr. 6, 64829 Darmstadt, Germany

Received October 29, 2008; Revised Manuscript Received November 27, 2008

ABSTRACT: Poly[bis(methoxy)phosphazene] (PBMP) is used as a model to investigate the backbone dynamics of polyphosphazenes approaching their glass transitions. Specifically, we study PBMP featuring deuterated methyl groups so that, as a consequence of fast rotation of the methyl groups, ^{2}H NMR probes the reorientation of their 3-fold symmetry axes and, thus, of the inorganic backbone. Combining ^{2}H NMR spin−lattice relaxation, line-shape, and stimulated-echo analyses, we follow the slowdown of the segmental motion upon cooling over a broad temperature/time range. Comparison of present and previous results provides no evidence that polymers featuring inorganic and organic backbones, respectively, show fundamentally different dynamical behaviors during vitrification. In particular, typical of glass-forming polymer melts, we find for the α-process of PBMP that its temperature dependence deviates from an Arrhenius law and its time dependence differs from a single-exponential function. ^{2}H NMR three-time correlation functions indicate that both homogeneous and heterogeneous dynamics contribute to the nonexponential relaxation. In addition, ^{2}H NMR spin−lattice relaxation and line-shape analyses reveal the existence of some large-angle anisotropic precursor motion in the moderately viscous melt, which may be a peculiarity of polyphosphazene.

I. Introduction

Today plastics play an important role in both everyday life and technological applications. Until now, the plastics market has been dominated by organic polymers, but inorganic polymers become more and more important. Inorganic polymers can overcome problems of organic polymers like the poor flexibility at low temperature, limited stability at high temperature, poor biomedical compatibility, and lack of thermal and/or electric conductivity. Also, they often exhibit a better fire resistance.[1,2] In addition to the well-known polysiloxanes (silicones), polyphosphazenes attract a great deal of attention due to many potential applications.[1,3]

Synthesis and characterization of polyphosphazenes were first reported in the 1960s by Allcock et al.[4−6] The general structure of polyphosphazenes is shown in Figure 1. The great variety of possible, mostly organic, substituents enables synthesis of polyphosphazenes with very different properties, which range from hydrophilic to hydrophobic, elastomer to glass, electric conductor to insulator, and so on. The main features of the inorganic backbone are fire resistance and high flexibility, leading to low glass transition temperatures T_g when substituents of moderate bulkiness are used.[1,2] Many scientific studies of polyphosphazenes focus on their applications as flame retardants or biomaterials, e.g., as drug delivery systems, implants, and protheses. Furthermore, polyphosphazenes are good candidates for the use as polymer electrolytes in rechargeable lithium ion batteries. For example, high ionic conductivities of 10^{-5} S/cm were reported for ion conducting membranes on the basis of poly[bis((methoxyethoxy)ethoxy)phosphazene].[7]

Further improvement of the material properties requires thorough knowledge about the thermodynamic, structural, and dynamic behaviors of polyphosphazenes. For a fundamental understanding, it is important to investigate the behaviors of the phosphorus−nitrogen backbone, i.e., to use small substituents, and to compare the results for inorganic and organic backbones. Recent work[8] utilized poly[bis(methoxy)phosphazene] (PBMP) as a model polymer to study thermodynamic and structural aspects. Here, the dynamics of this polyphosphazene are characterized in some detail using ^{2}H NMR. In the studied PBMP-d_6, deuterated methyl groups are directly bound to the polymer backbone (R = CD_3) so that they can be employed as probes for the backbone dynamics (see below). In addition to temperature-dependent ^{2}H NMR spin−lattice relaxation (SLR) and line-shape (LS) analyses, we perform ^{2}H NMR stimulated-echo (STE) experiments, providing straightforward access to multitime correlation functions of the polymer segmental motion.[9−14] The latter yield detailed information about the complex dynamics in polymer melts, which manifest themselves in nonexponential relaxation. While two-time correlation functions (2T-CF) allow us to measure the correlation time τ and to determine the extent of deviations from single-exponential behavior, three-time correlation functions (3T-CF) enable quantitative analysis of the origin of the nonexponentiality.

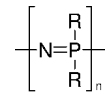

Figure 1. Polyphosphazene. R = organic, metalorganic, or inorganic substituent. In our case, R = CD_3 and $n \approx 15\,000$.

II. Theory

A. Basics of ^{2}H NMR Experiments. In solid-state ^{2}H NMR ($I = 1$), first-order quadrupolar interaction is the dominant internal interaction. It results from the interaction of the nuclear quadrupole moment with the electric field gradient (EFG) at the nuclear site, leading to a frequency shift ω_Q with respect to the Larmor frequency ω_0. This shift is probed in the experiment. In our case of PBMP-d_6, the deuterons are located in methyl groups. Because of fast methyl group rotation at the studied

* To whom correspondence should be addressed.

10.1021/ma802421e CCC: $40.75
Published on Web 12/23/2008

temperatures, the EFG tensor is preaveraged. The principal z-axis of the averaged tensor points along the direction of the 3-fold symmetry axis of this unit. Then, the quadrupolar frequency is given by[9−14]

$$\omega_Q(\theta) = \pm\frac{\delta}{2}(3\cos^2\theta - 1) \quad (1)$$

Here, δ denotes the anisotropy parameter of the averaged tensor and θ is the angle between the C_3-axis of the methyl group and the external static magnetic flux density B_0. The $\pm$ signs in eq 1 correspond to two allowed transitions between three Zeeman levels. Because of the dependence of the quadrupolar frequency on the orientation of the C_3-axis, reorientations of this axis render ω_Q time dependent. Therefore, ^{2}H NMR is a powerful tool to study the rotational motion of the 3-fold axes. Furthermore, since the methyl groups are directly bound to the polyphosphazene main chain, the reorientations of the C_3-axes probe the dynamics of the inorganic backbone, which we are interested in. We note that, in ^{31}P NMR studies of the backbone dynamics, strong homonuclear dipole−dipole interactions interfere with straightforward data analysis.

B. Spin−lattice Relaxation Analysis. The ^{2}H SLR time T_1 depends on the spectral density of the rotational dynamics. When the temperature is increased and molecular dynamics become faster, T_1 decreases at low temperatures ($\omega_0\tau \gg 0.6$), while it increases at high temperatures ($\omega_0\tau \ll 0.6$). A T_1 minimum is observed for $\omega_0\tau = 0.6$,[15] i.e., for τ on the order of 1 ns. In studies on molecular and polymeric glass-formers, ^{2}H SLR was found to become nonexponential when cooling toward the glass transition temperature, T_g.[11,16] In the case of ^{2}H NMR, such nonexponential SLR can be traced back to the existence of a distribution of correlation times $G(\log\tau)$, leading to a distribution of SLR times $V(T_1)$.[11] Then, SLR can be characterized by either the mean SLR time $\langle T_1\rangle$ or the mean SLR rate $\langle 1/T_1\rangle$, where $\langle T_1\rangle > \langle 1/T_1\rangle^{-1}$.

C. Line-Shape Analysis. In our case of an amorphous sample, the anisotropy of the quadrupolar interaction in combination with the powder average results in broad ^{2}H NMR spectra with a characteristic LS called the Pake spectrum. These broad rigid-lattice spectra are observed when the limit of slow motion is reached at low temperatures, i.e., when the correlation time exceeds the inverse spectral width, $\tau \gg 1/\delta$. Increasing the temperature, motional narrowing sets in and the spectra collapse when τ becomes comparable to $1/\delta$. Motionally averaged spectra result in the limit of fast motion, $\tau \ll 1/\delta$. Fast isotropic reorientations result in narrow Lorentzian lines. When a broad distribution $G(\log\tau)$ exists so that there are fast ($\tau \ll 1/\delta$) and slow ($\tau \gg 1/\delta$) polymer segments at a given temperature, the LS can be described as a superposition of a broad Pake spectrum and a motionally narrowed line. Such spectra have been called two-phase spectra.[18]

D. Two-Time Correlation Functions. ^{2}H NMR STE spectroscopy has proved a powerful tool to study molecular dynamics with correlation times in the range of 10 μs $\leq \tau \leq$ 1s.[9−14] In these experiments, the three-pulse sequence $P_1-t_p-P_2-t_m-P_3-t_p$ is utilized to correlate the quadrupolar frequencies during two short evolution times $t_p \ll \tau$, which are separated by a longer mixing time $t_m \approx \tau$ so that molecular rotational jumps can alter the value of ω_Q during the latter period. When appropriate pulse lengths and phases are used, measuring the height of the stimulated echo for various t_m, but constant t_p, provides access to the 2T-CF[9−14]

$$E_2^{ss}(t_m;t_p) = \langle \sin[\omega_1 t_p]\sin[\omega_2 t_p]\rangle \quad (2)$$

$$E_2^{cc}(t_m;t_p) = \langle \cos[\omega_1 t_p]\cos[\omega_2 t_p]\rangle \quad (3)$$

Here, the brackets $\langle ...\rangle$ denote the ensemble average. We see that the frequencies at two times, $\omega_1 \equiv \omega_Q(0)$ and $\omega_2 \equiv \omega_Q(t_m)$, are correlated. Hence, the correlation functions $E_2^x(t_m)$ (x = cc, ss) decay when molecular reorientation during the mixing time leads to $\omega_1 \neq \omega_2$.

SLR can lead to additional damping of the ^{2}H NMR STE decays, rendering correction for relaxation effects useful. In the case of E_2^{cc}, the decay of Zeeman order, which exists during the mixing time of this experiment, can be determined in a regular SLR measurement so that division by the SLR function often enables a removal of relaxation effects. Therefore, we show data E_2^{cc} that have been corrected for SLR throughout this paper. In the case of E_2^{ss}, the decay of alignment order, which is present during the mixing time of this experiment, is not accessible in an independent measurement, hampering correction for relaxation effects. Therefore, the time window of E_2^{ss} is more restricted.

E. Three-Time Correlation Functions. Nonexponential relaxation of polymer melts can be explained within two fundamentally different scenarios. In the limit of purely homogeneous dynamics, a distribution of correlation times is absent, and all polymer segments obey the same correlation function, which is intrinsically nonexponential, e.g., due to correlated back-and-forth motion. In the limit of purely heterogeneous dynamics, correlated back-and-forth motion is absent and all polymer segments exhibit an exponential correlation function, but a distribution of correlation times exists. Generally, one expects both homogeneous and heterogeneous contributions to the nonexponentiality so that it is important to analyze their relevances. Such analysis is possible on the basis of ^{2}H NMR 3T-CF.[9,11]

For a measurement of ^{2}H NMR 3T-CF, we apply appropriate seven-pulse sequences, enabling correlation of the quadrupolar frequencies ω_1, ω_2, ω_3, and ω_4 during four evolution times of equal length t_p, which are separated by the mixing times t_{m1}, t_{m2}, and t_{m3}.[9,11,19] These pulse sequences can be regarded as two successive STE experiments. The first one with mixing time t_{m1} is followed after a time t_{m2} by the second one with mixing time t_{m3}. For analysis of nonexponential relaxation, it is useful to vary t_{m3} for $t_{m1} \approx \tau$ and $t_{m2} \ll \tau$.[11,12,20−23] Then, $\omega_2 = \omega_3 \equiv \omega_{2,3}$ and a 3T-CF results. Specifically, it is possible to record

$$E_3^{cc}(t_{m3};t_{m1}) = \langle \cos[(\omega_{2,3} - \omega_1)t_p]\cos(\omega_{2,3}t_p)\cos(\omega_4 t_p)\rangle \quad (4)$$

In previous works,[22−24] the interpretation of E_3^{cc} was discussed in some detail. Briefly, in the limit of purely heterogeneous dynamics, the first STE experiment acts as a dynamic filter selecting the slow ($\tau > t_{m1}$) polymer segments from the distribution of correlation times because these segments are static during the corresponding mixing time t_{m1} and show $\omega_1 = \omega_{2,3}$. Directly afterward ($t_{m2} \ll \tau$), the correlation function is measured exclusively for the selected subensemble of slow segments in the second STE experiment by variation of the mixing time t_{m3}. The correlation function of this slow subensemble, E_3^{cc}, decays more slowly than that of the whole ensemble, E_2^{cc}. More precisely, in the limit of purely heterogeneous dynamics, it is possible to calculate a prediction for the 3T-CF based on a knowledge of the 2T-CF according to[11,22−24]

$$E_3^{het}(t_{m3};t_{m1}) = E_2(t_{m1} + t_{m3}) \quad (5)$$

In the limit of purely homogeneous dynamics, a distribution $G(\log\tau)$ is absent, impeding selection of a dynamically distinguishable subensemble by application of a dynamic filter

during the first STE experiment. However, correlated backward jumps can restore the initial resonance frequency during the experiment. In recent work,[22,23] detailed consideration of these effects showed that, in the limit of purely homogeneous dynamics, it is possible to compute a prediction for the 3T-CF based on a knowledge of the 2T-CF according to

$$E_3^{\mathrm{hom}}(t_{m3};t_{m1}) = \frac{1}{2}[E_2(t_{m1})E_2(t_{m3}) + E_2(t_{m1} + t_{m3})] \qquad (6)$$

Therefore, comparison of the experimental data E_3^{cc} with the predictions E_3^{het} and E_3^{hom} enables determination of the relevance of heterogeneous and homogeneous contributions to the nonexponential relaxation.

The correlation functions in eqs 2−6 are not normalized. Throughout this paper, we denote the normalized analogues as F_2^{ss}, F_2^{cc},..., and F_3^{hom}. For example, $F_3^{cc}(t_{m3}; t_{m1}) = E_3^{cc}(t_{m3}; t_{m1})/E_3^{cc}(0; t_{m1})$.

III. Experimental Section

Synthesis and characterization of the studied PBMP-d_6 were described in ref 8. A molecular weight of $M_w = 1.04 \times 10^5$ g/mol and a glass transition temperature of $T_g = 191$ K were reported. The present ^{2}H NMR experiments were performed on a Bruker DSX 500 spectrometer working at a Larmor frequency of $\omega_0 = 2\pi \times 76.8$ MHz. A static Bruker probe was used, resulting in 90° pulse lengths between 2.2 and 2.4 μs. To adjust the sample temperature, a Bruker VT 3000 heating unit was employed. To remove deviations between set and actual temperature within an uncertainty of ±1.5 K, a temperature calibration with ^{207}Pb NMR of lead nitrate was done.[25] The solid-echo pulse sequence $90°_x-t_p-90°_y$ was used to acquire ^{2}H NMR spectra. SLR times were measured utilizing the saturation recovery pulse sequence at lower temperatures and the inversion recovery pulse sequence at higher temperatures combined with a solid echo for detection. To record ^{2}H NMR 2T- and 3T-CF, we applied appropriate three-pulse and seven-pulse sequences, respectively.[9−12,14]

IV. Results

First, we perform SLR measurements to obtain information about polymer dynamics with $\tau \approx 1/\omega_0$. For polymer melts, distributions $G(\log \tau)$ can result in distributions of SLR times and, hence, in nonexponential SLR. For PBMP, we find exponential SLR above 210 K, implying that the structural relaxation or, equivalently, the α-process of the polymer melt averages over any distribution $V(T_1)$.[11] In other words, each deuteron samples a representative set of local environments on the time scale of SLR, which is a typical finding in studies on the α-process of glass-forming liquids. As a consequence, the relaxation function is given by $\Phi(t) \equiv 1 - M_z(t)/M_0 = \exp(-\langle 1/T_1\rangle t)$ and, hence, $T_1 = \langle 1/T_1\rangle^{-1}$.[17] In Figure 2, it is evident that T_1 is a minimum at about 255 K, indicating $\omega_0\tau_\alpha \approx 0.6$ for the correlation time of the α-process. On the low-temperature side of the T_1 minimum, we see a shoulder at $T \approx 1.1T_g$. While shoulders at $T \approx T_g$ are common to glass-forming liquids,[11] observation of such feature at $T > T_g$ implies that, in addition to the structural relaxation, PBMP exhibits a faster secondary relaxation, which starts to govern SLR in the vicinity of the glass transition. For convenience, we refer to the latter relaxation as a β-process. However, this does not imply that it is related to the β-process of mode-coupling theory[26] or to the β-process of Johari and Goldstein.[27]

When further cooling PBMP toward T_g, SLR becomes nonexponential. Thus, in the vicinity of T_g, the α-process is too slow to establish ergodicity on the time scale of SLR so that an underlying distribution $V(T_1)$ becomes apparent. Then, the mean SLR time $\langle T_1\rangle$ and the inverse mean SLR rate $\langle 1/T_1\rangle^{-1}$ differ.[17] To determine the mean SLR time, we interpolate

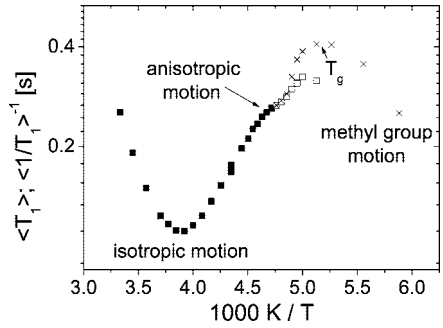

Figure 2. Temperature-dependent ^{2}H NMR SLR times T_1 of PBMP-d_6. At temperatures $T < 210$ K, we characterize the nonexponential SLR using both the mean SLR time $\langle T_1\rangle$ (crosses), as obtained from fits to eq 7, and the inverse mean relaxation rate $\langle 1/T_1\rangle^{-1}$ (open squares), as determined from the initial ($t \rightarrow 0$) slope of the relaxation function.

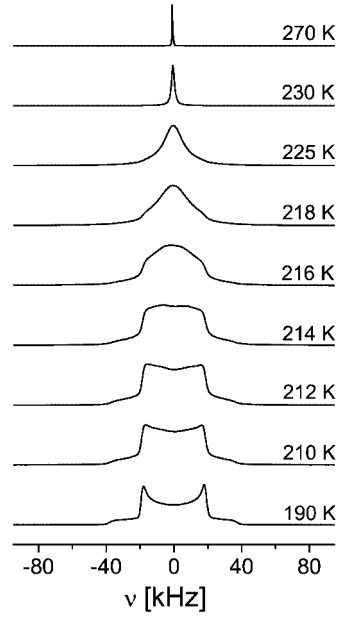

Figure 3. Temperature-dependent ^{2}H NMR spectra of PBMP-d_6.

the relaxation function with a Kohlrausch−Williams−Watts (KWW) function

$$\Phi(t) = \exp\left[-\left(\frac{t}{T_1}\right)^{\beta}\right] \qquad (7)$$

yielding stretching parameters that decrease from $\beta = 1$ to $\beta = 0.7$ when T_g is approached and use the Γ function to obtain $\langle T_1\rangle = \int_0^\infty \Phi(t)\, dt = (T_1/\beta)\Gamma(1/\beta)$. The mean SLR rate $\langle 1/T_1\rangle$ can be extracted from the initial slope of $\Phi(t)$.[17] In Figure 2, we see that the temperature dependence of $\langle 1/T_1\rangle^{-1}$ continues that found in the region of exponential SLR, as expected since the rate average is probed in both temperature regimes. By contrast, $\langle T_1\rangle$ shows a stronger increase. It was shown[17] that this effect does not result from molecular dynamics, but rather from a crossover between rate and time average ($\langle T_1\rangle > \langle 1/T_1\rangle^{-1}$). Below T_g, T_1 decreases with decreasing temperature, indicating that fast methyl group reorientation ($\omega_0\tau_{CH_3} \ll 0.6$) starts to govern SLR.

Temperature-dependent ^{2}H NMR spectra are shown in Figure 3. At $T = 190$ K, a Pake pattern is found. The observed line is a factor of 3 smaller than that of static C−D bonds,[9] indicating that fast methyl group rotation leads to a preaveraged EFG tensor, consistent with the results of SLR analysis. Therefore,

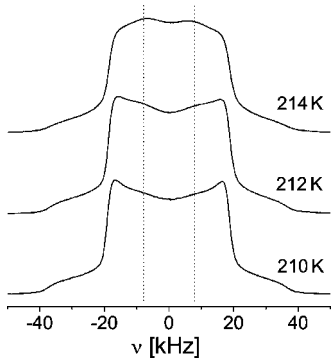

Figure 4. Enlargement of the ^{2}H NMR spectra at $T = 210-214$ K. The dotted lines are meant to aid identification of additional intensity at ± 8 kHz.

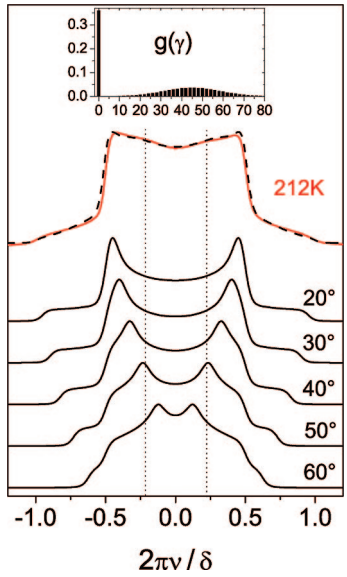

Figure 5. Measured (solid line) and simulated (dashed line) spectrum at 212 K. The dotted lines mark the location of additional spectral intensity. The inset shows the distribution of jump angles, $g(\gamma)$, used in the simulation; see text for details. In the bottom part, simulated spectra for fast ($\tau \ll 1/\delta$) two-site jumps about various jump angles γ are compiled.

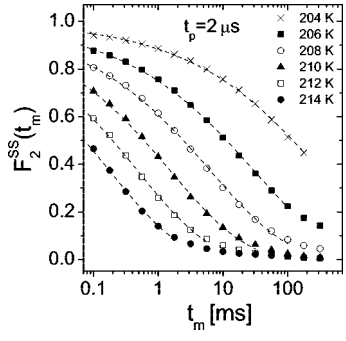

Figure 6. Correlation functions $F_2^{ss}(t_m; t_p = 2\ \mu s)$ at various temperatures. Fits to eq 7 are included as dashed lines.

at all studied temperatures, we probe the rotational jumps of the 3-fold methyl group axis. Hence, the Pake spectrum at $T =$ 190 K shows that the limit of slow motion is fulfilled for the reorientation of this axis and, thus, for the α-process of the backbone, i.e., $\tau_\alpha \gg 1/\delta$. At $T \geq 230$ K, observation of a Lorentzian demonstrates the existence of fast isotropic motion so that $\tau_\alpha \ll 1/\delta$. The collapse of the Pake spectrum occurs at about 220 K, indicating $\tau_\alpha \approx 1/\delta \approx 4\ \mu s$. However, closer

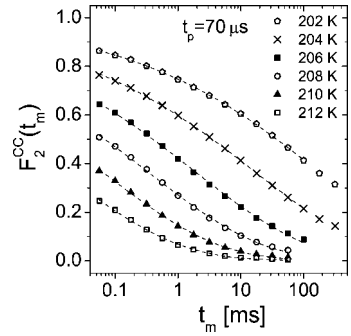

Figure 7. Correlation functions $F_2^{cc}(t_m; t_p = 70\ \mu s)$ at various temperatures. Fits to eq 7 are included as dashed lines.

inspection reveals that, in the range 215−225 K, the spectra can be described by a superposition of a narrow and a broad LS component. Thus, two-phase spectra are found, showing that correlation times $\tau_\alpha \ll 1/\delta$ and $\tau_\alpha \gg 1/\delta$ coexist; i.e., there is a distribution $G(\log \tau_\alpha)$.

In the temperature range 205−215 K, a different type of LS changes is observed. In Figure 4, we have a closer look at the spectra between 210 and 214 K. We see additional intensity at about ± 8 kHz, which is higher for higher temperatures, while the outer edges of the spectra are hardly affected. These findings suggest that a β-process does not only manifest itself in the SLR but also in the LS. On the basis of the LS effects, we can identify the β-process with an anisotropic motion. For example, the additional spectral intensity at ± 8 kHz can be rationalized when we assume fast ($\tau_\beta \ll 1/\delta$) two-site jumps. In Figure 5, we show calculated spectra resulting from two-site jumps about different jump angles γ in the limit of fast motion. Evidently, the positions of the horns strongly depend on the jump angle. For $\gamma \approx 50°$, they are located at about ± 8 kHz, where the additional intensity is found in the experimental spectra. However, using a single correlation time τ_β and a single jump angle γ, it is not possible to reproduce the experimental data. Rather, we have to use distributions. Specifically, we have to assume that a distribution $G(\log \tau_\beta)$ exists so that segments exhibiting $\tau_\beta \gg 1/\delta$ and $\tau_\beta \ll 1/\delta$ yield a Pake spectrum and an anisotropically averaged spectrum, respectively. Also, a distribution of jump angles $g(\gamma)$ is necessary to smear out the intensities resulting from the horns of the latter LS component. In Figure 4, we see that such approach enables good reproduction of the experimental spectrum at $T = 212$ K. In the used distribution $g(\gamma)$, the contribution at $\gamma = 0°$ can be identified with the fraction of polymer segments showing $\tau_\beta \gg 1/\delta$ at this temperature. On the basis of our results, we cannot distinguish whether these segments are truly immobile or whether they move just too slow on the experimental time scale, i.e., whether the distribution $G(\log \tau_\beta)$ is bimodal or continuous. In any case, the temperature dependence of the LS indicates that the fraction of segments showing fast anisotropic motion on the experimental time scale increases with increasing temperature, at least between 210 and 214 K. Although the two-site jump model allows us successful LS analysis, we expect that there are other models of anisotropic motion, e.g., rotational diffusion on a cone, which enable a comparable reproduction of the experimental spectra.

Further insights into the segmental motion of PBMP are available when we measure 2T-CF in ^{2}H STE experiments. In Figures 6 and 7, we present $F_2^{ss}(t_m; t_p = 2\ \mu s)$ and $F_2^{cc}(t_m; t_p = 70\ \mu s)$, respectively. The former data map out the rotational

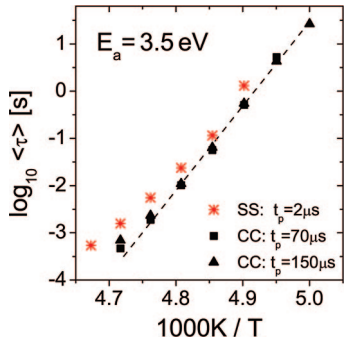

Figure 8. Mean correlation times $\langle\tau\rangle$ from $F_2^{ss}(t_m; t_p = 2\ \mu s)$, $F_2^{cc}(t_m; t_p = 70\ \mu s)$, and $F_2^{cc}(t_m; t_p = 150\ \mu s)$. The dashed line is a fit of the latter data to an Arrhenius law.

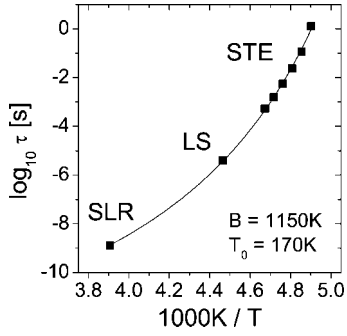

Figure 9. Correlation times determined for PBMP-d_6 in various ^{2}H NMR experiments. Specifically, $\langle\tau\rangle$ from STE experiments (F_2^{ss}) is compared with $\tau = 4.0\ \mu s$ and $\tau = 1.3$ ns from LS and SLR analyses, respectively. All data are fitted to a VFT law (solid line).

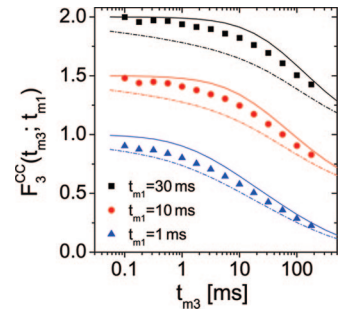

Figure 10. $F_3^{cc}(t_{m3}; t_{m1} = 1, 10, 30$ ms) of PBMP-d_6 at 204 K. The respective theoretical predictions for the homogeneous limit (dashed lines) and the heterogeneous limit (solid lines) are included. For clarity, the data corresponding to $t_{m1} = 10$ ms and $t_{m1} = 30$ ms are shifted upward by 0.5 and 1.0, respectively.

correlation function F_2 of the second Legendre polynomial $P_2(\cos\theta)$ since, for $t_p \rightarrow 0$,

$$F_2^{ss}(t_m) \propto \langle\omega_1\omega_2\rangle \propto \langle P_2[\cos\theta(0)]P_2[\cos\theta(t_m)]\rangle \propto F_2(t_m)$$

Both F^{ss}_2 and F^{cc}_2 exhibit nonexponential decays, which strongly depend on temperature. For quantitative analysis, we fit the decays to a KWW function. We obtain small stretching parameters $\beta = 0.23-0.24$, indicating pronounced deviations from simple single-exponential behavior. The mean correlation times calculated from the fit parameters according to $\langle\tau\rangle = (\tau/\beta)\Gamma(1/\beta)$ are displayed in Figures 8 and 9. Interpolation with an Arrhenius law yields a high apparent activation energy of $E_a = 3.5$ eV ($E_a = 340$ kJ/mol). However, if we combine the correlation times from the STE experiments with that from SLR and LS analyses, clear deviations from an Arrhenius law are evident (see Figure 6). As expected for glass-forming polymer melts, all data are consistently described by the Vogel−Fulcher−Tammann (VFT) equation

$$\tau = \tau_0 \exp\left[\frac{B}{T - T_0}\right] \quad (8)$$

where $B = 1150$ K and $T_0 = 170$ K. In previous studies, a VFT temperature dependence was also observed for the α-process of polyphosphazenes featuring bulkier side groups,[28−30] e.g., for poly[bis(trifluorethoxy)phosphazene] (PFEP). Extrapolating the present VFT fit to lower temperatures, a correlation time of $\tau \approx 100$ s is reached in the vicinity of the calorimetric glass transition, $T_g = 191$ K,[8] confirming that the STE experiments probe the α-process. In agreement with this conclusion, reinspection of Figure 6 shows that the observed dynamical process leads to a complete decay of F_2, as expected for isotropic reorientation associated with the α-process, while restricted reorientation typical of a β-process would leave a finite residual correlation at $t_m \gg \tau$. Hence, unlike SLR and LS studies at higher temperatures, STE studies do not provide evidence for the existence of a faster β-process at lower temperatures. For PFEP, a β-process was observed below T_g, but not attributed to main chain dynamics, which is probed in the present study, but rather to some motion of the flexible side chain of this polyphosphazene.[28,29]

In STE experiments, variation of the evolution time t_p enables adjustment of the angular resolution.[11,31] Specifically, the sensitivity to small changes of ω_Q and, thus, to small angular displacements is higher for longer t_p (see eqs 2 and 3). Therefore, the dependence of the STE decays on the evolution time can be used to extract information about the geometry of the motion. In particular, the dependence $\tau(t_p)$ yields insight into the typical jump angles during an isotropic reorientation process.[11] While τ is independent of t_p for isotropic random jumps, i.e., if the jump leads to a random new position on the unit sphere, $\tau \propto t_p^{-2}$ for isotropic rotational diffusion. In Figure 8, we see that a significant extension of the evolution time leads to a moderate decrease of τ. This finding shows that neither of the limiting cases of large-angle and small-angle motion applies to the α-process of PBMP. Consistently, mean jump angles of about 10° resulted from more detailed STE analyses for various molecular and polymeric glass-forming liquids.[11,12]

The pronounced nonexponentiality of the 2T-CF can be due to homogeneous or heterogeneous dynamics (see section IIE). For a quantitative analysis of its origin, we measure 3T-CF. In Figure 10, we compare $F_3^{cc}(t_{m3}; t_{m1})$ of PBMP at $T = 204$ K with the corresponding predictions for purely heterogeneous and purely homogeneous dynamics, which were calculated from the 2T-CF using eqs 5 and 6. For various mixing times t_{m1}, i.e., for diverse dynamic filters, the experimental data lie between the two predictions, indicating that heterogeneous and homogeneous contributions are of comparable relevance.

V. Discussion and Conclusion

We demonstrated that PBMP exhibits a dynamical behavior typical of glass-forming polymer melts.[9] Specifically, a combination of ^{2}H NMR SLR, LS, and STE analyses showed that the temperature dependence of the α-process is not described by an Arrhenius law, but rather by a VFT law. Also, the loss of orientational correlation due to the α-process is nonexponential. The nonexponentiality results from homogeneous and heterogeneous contributions; i.e., a distribution $G(\log\tau_\alpha)$ exists. In particular, the results of the present ^{2}H NMR 3T-CF study on PBMP resemble that of previous work on poly(propylene oxide).[23] Finally, molecular reorientation is not described by the models of isotropic random jumps or isotropic rotational diffusion, but it involves rotational jumps about moderate angles, as was found for a number of glass-forming liquids.[11] Hence, the present results for a polymer featuring an inorganic backbone

provide no evidence that the overall phenomenology of the glass transition phenomenon depends on the specific backbone architecture.

Nevertheless, there are some differences. The phosphorus−nitrogen backbone of polyphosphazenes is highly flexible. Therefore, polyphosphazenes exhibit fast segmental motion at ambient temperatures, rendering them promising materials for a use in polymer electrolytes, where fast polymer dynamics is required to facilitate fast ion transport. The present ^{2}H NMR SLR and LS studies on PBMP imply that at least a significant fraction of segments exhibits an anisotropic motion preceding the structural relaxation in the moderately viscous melt. The origin of this behavior is not yet clear. Our ^{2}H NMR STE measurements provide no evidence for the existence of such motion in the highly viscous melt, suggesting that the observed dynamics is not a typical β-process[27] because such secondary relaxations persist even in the glassy state.

Acknowledgment. We thank H.-D. Wiemhöfer for providing us with PBMP-d_6. Funding of the Deutsche Forschungsgemeinschaft through the Sonderforschungsbereich 458 is gratefully acknowledged.

References and Notes

(1) Gleria, M.; DeJaeger, R. *Top. Curr. Chem.* **2005**, *250*, 165.
(2) Lawson, D. F.; Cheng, T. C. *Fire Res. (Lausanne)* **1977/78**, *223*, 223.
(3) Honarkar, H.; Rahimi, A. *Chem. Mon.* **2007**, *138*, 923.
(4) Allcock, H. R.; Kugel, R. L. *Am. Chem. Soc.* **1965**, *87*, 4216.
(5) Allcock, H. R.; Kugel, R. L.; Valan, K. J. *Inorg. Chem.* **1966**, *5*, 1709.
(6) Allcock, H. R.; Kugel, R. L. *Inorg. Chem.* **1966**, *5*, 1716.
(7) Blonsky, P. M.; Shriver, D. F.; Austin, P.; Allcock, H. R. *J. Am. Chem. Soc.* **1984**, *106*, 6854.
(8) Karatas, Y.; Pyckhout-Hintzen, W.; Zorn, R.; Wiemhöfer, H.-D. *Macromolecules* **2008**, *41*, 2212.
(9) Schmidt-Rohr, K.; Spiess, H. W. *Multidimensional Solid State NMR and Polymers*; Academic Press: London, 1994.
(10) Duer, M. J. *Annu. Rep. NMR Spectrosc.* **2000**, *43*, 1.
(11) Böhmer, R.; Diezemann, G.; Hinze, G.; Rössler, E. *Prog. Nucl. Magn. Reson. Spectrosc.* **2001**, *39*, 191.
(12) Böhmer, R.; Kremer, F. In *Broadband Dielectric Spectroscopy*; Springer: Berlin, 2002.
(13) Vogel, M.; Medick, P.; Rössler, E. *Annu. Rep. NMR Spectrosc.* **2005**, *56*, 231.
(14) deAzevedo, E. R.; Bonagamba, T. J.; Reichert, D. *Prog. Nucl. Magn. Reson. Spectrosc.* **2005**, *47*, 137.
(15) Bloembergen, N.; Purcell, E. M.; Pound, R. V. *Phys. Rev.* **1948**, *73*, 679.
(16) Schnauss, W.; Fujara, F.; Hartmann, K.; Sillescu, H. *Chem. Phys. Lett.* **1990**, *166*, 381.
(17) Geil, B.; Hinze, G. *Chem. Phys. Lett.* **1993**, *216*, 51.
(18) Rössler, E.; Taupitz, M.; Börner, K.; Schulz, M.; Vieth, H.-M. *J. Chem. Phys.* **1990**, *92*, 5847.
(19) Hinze, G.; Böhmer, R.; Diezemann, G.; Sillescu, H. *J. Magn. Reson.* **1998**, *131*, 218.
(20) Tracht, U.; Heuer, A.; Spiess, H. W. *J. Non-Cryst. Solids* **1998**, *27*, 235–237.
(21) Böhmer, R.; Hinze, G.; Diezemann, G.; Sillescu, H. *J. Chem. Phys.* **1998**, *108*, 890.
(22) Vogel, M.; Brinkmann, C.; Eckert, H.; Heuer, A. *Phys. Rev. B* **2004**, *69*, 094302.
(23) Vogel, M.; Torbrügge, T. *J. Chem. Phys.* **2007**, *126*, 204902.
(24) Heuer, A.; Tracht, U.; Kuebler, S. C.; Spiess, H. W. *J. Mol. Struct.* **1999**, *479*, 251.
(25) Takahashi, T.; Kawashima, H.; Sugisawa, H.; Baba, T. *Solid State Nucl. Magn. Reson.* **1999**, *15*, 119.
(26) Götze, W.; Sjögren, L. *Rep. Prog. Phys.* **1992**, *55*, 241.
(27) Johari, G. P.; Goldstein, M. *J. Chem. Phys.* **1970**, *53*, 2372.
(28) Moriya, K.; Nishibe, Y.; Yano, S. *Macromol. Chem. Phys.* **1994**, *195*, 713.
(29) Van Mourik, P.; Veldman, E.; Norder, B.; Van Turnhout, J.; Wübbenhorst, M. *J. Mater. Sci.* **2005**, *40*, 1661.
(30) Kumar, K.; Robertson, C. G.; Pawlus, S.; Hahn, S. F.; Sokolov, A. P. *Macromolecules* **2008**, *41*, 7232.
(31) Fleischer, G.; Fujara, F. *NMR - Basic Principles and Progress*; Springer: Berlin, 1994; Vol. *30*, p 159.

MA802421E